

Observations of magnetic anomaly signatures in Mars Express ASPERA-3 ELS data

Y. Soobiah^{a,*}, A.J. Coates^a, D.R. Linder^a, D. O. Kataria^a, J.D. Winningham^b, R.A. Frahm^b,
J.R. Sharber^b, J. Scherrer^b, S. Barabash^c, R. Lundin^c, M. Holmström^c, H. Andersson^c, M.
Yamauchi^c, A. Grigoriev^c, E. Kallio^d, H Koskinen^{d,e}, T. Säles^d, P. Riihela^d, W. Schmidt^d,
J. Kozyra^f, J. Luhmann^g, E. Roelof^h, D. Williams^h, S. Livi^h, C. C. Curtisⁱ, K.C. Hsiehⁱ, B.
R. Sandelⁱ, M. Grande^j, M. Carter^j, J.-A. Sauvaud^k, A. Fedorov^k, J.-J. Thocaven^k, S.
McKenna-Lawler^l, S. Orsini^m, R. Cerulli-Irelli^m, M. Maggi^m, P. Wurzⁿ, P. Bochslerⁿ, N.
Krupp^o, J. Woch^o, M. Fraenz^o & K. Asamura^p, C. Dierker^q.

^aMullard Space Science Laboratory, University College London, Surrey RH5
6NT, UK

*Corresponding Author E-mail address: yijs@mssl.ucl.ac.uk

^bSouthwest Research Institute, San Antonio, TX 7228-0510, USA.

^cSwedish Institute of Space Physics, Box 812, S-98 128, Kiruna, Sweden.

^dFinnish Meteorological Institute, Box 503 FIN-00101 Helsinki, Finland.

^eDepartment of Physical Sciences, University of Helsinki, Box 64 FIN-00014, Helsinki,
Finland

^fSpace Physics Research Laboratory, University of Michigan, Ann Arbor, MI 48109-2143,
USA

^gSpace Science Laboratory, University of California in Berkeley, Berkeley, CA 94720-
7450, USA

^hApplied Physics Laboratory, Johns Hopkins University, Laurel, MD 20723-6099, USA

ⁱUniversity of Arizona, Tucson, AZ 85721, USA

^jRutherford Appleton Laboratory, Chilton, Didcot, Oxfordshire OX11 0QX, UK

^kCentre d'Etude Spatiale des Rayonnements, BP-4346, F-31028 Toulouse, France

^lSpace Technology Ireland, National University of Ireland, Maynooth, Co. Kildare, Ireland

^mInstituto di Fisica dello Spazio Interplanetari, I-00133 Rome, Italy

ⁿUniversity of Bern, Physikalisches Institut, CH-3012 Bern Switzerland

^oMax-Planck-Institut für Aeronomie, D-37191 Katlenburg-Lindau, German

^pInstitute of Space and Astronautical Science, 3-1-1 Yoshinodai, Sagamichara, Japan

^qTechnical University of Braunschweig, Hans-Sommer-Strasse 66, D-38106 Braunschweig,
Germany

Pages: 21

Table: 0

Figures: 8

Proposed Running Head: Magnetic anomaly signatures in MEX ASPERA-3 ELS data

Editorial correspondence to:

Mr Yasir Soobiah

Mullard Space Science Laboratory

Holmbury St Mary

Dorking

Surrey

United Kingdom

RH5 6NT

Phone: 01483 204146

Fax: 01483 278312

E-mail address: yijs@mssl.ucl.ac.uk

ABSTRACT

Mars Express (MEX) Analyzer of Space Plasmas and Energetic Atoms (ASPERA-3) data is providing insights into atmospheric loss on Mars via the solar wind interaction. This process is influenced by both the interplanetary magnetic field (IMF) in the solar wind and by the magnetic ‘anomaly’ regions of the Martian crust. We analyse observations from the ASPERA-3 Electron Spectrometer near to such crustal anomalies. We find that the electrons near remanent magnetic fields either increase in flux to form intensified signatures or significantly reduce in flux to form plasma voids. We suggest that cusps intervening neighbouring magnetic anomalies may provide a location for enhanced escape of planetary plasma. Initial statistical analysis shows that intensified signatures are mainly a dayside phenomenon whereas voids are a feature of the night hemisphere.

Key Words: Magnetic Fields, Solar Wind, Mars

1. INTRODUCTION

Before the arrival of Mars Global Surveyor (MGS) it was impossible to confidently establish whether or not there are significant planetary magnetic fields at Mars. The observations onboard Phobos 2 indicated that the dipolar component of the planetary fields is less than 50 nT at the surface of Mars. The interaction of Mars with the solar wind was interpreted to be ‘Venus-like’ (where the ionosphere and atmosphere contribute to the solar wind obstacle). In such an interaction, part of the interaction region becomes “mass loaded” with heavy (O_2^+ , $H_2O_2^+$, CO^+) and light (H^+ and He^+) ions, formed due to the ionization of neutral exospheric particles. In this sense, the interaction is similar to the comet-solar wind interaction. There is the possibility of escape for those ions with large enough gyro radii that do not re-enter the atmosphere. Those that penetrate the atmosphere may form further ions via sputtering.

The MGS Magnetometer/Electron Reflectometer (MAG/ER) [1997 to present] discovered strongly magnetized regions in the crust of Mars (Acuña et al., 1998) indicating the presence near the Martian surface of localised magnetic crustal ‘anomalies’. MAG/ER confirmed that if an internal dipole field were still present it would be extremely weak; the maximum Mars dipole was found to be $\sim 2 \times 10^{17}$ A/m² (Acuña et al., 2001), with an associated field at the equator of 0.5 nT.

The present picture of the Mars-solar wind interaction is that the bow shock forms upstream from the planet since a conducting obstacle such as the ionosphere deflects solar wind plasma, then just downstream of the bow shock the IMF starts to drape and forms the so-

called magnetic pile-up boundary (MPB) (e.g. Bertucci et al., 2004, Brain et al., 2003). At the top of the region of planetary plasma is a second boundary, the photoelectron boundary (PEB), which is the upper altitude limit of planetary photoelectrons and the lower altitude limit of shocked magnetosheath electrons; the PEB was detected in both MGS and Mars Express data.

This interaction and the associated boundaries are significantly affected by crustal magnetic field sources, up to altitudes of 1300-1400 km above the strongest crustal anomalies. In addition, individual crustal sources are magnetically connected to regions of oppositely directed magnetic field via arched field lines. This interaction is also influenced by external conditions (e.g. Brain et al., 2003), since the changing solar wind controls the magnetic field orientation and topology over some crustal sources on the dayside. This may lead to magnetic reconnection at the outer part of these ‘mini-magnetospheres’. Therefore, Mars presents an irregularly shaped, weakly magnetic (on a small scale) and time variable obstacle to the solar wind.

There is already a large amount of work and literature on observations made by the MGS Electron Reflectometer (ER) [see the book “Mars’ Magnetism and its interaction with the Solar Wind” (Winterhalter, Acuña and Zakharov, 2004) and all references therein]. Our results are specifically relevant to MGS MAG/ER observations (Mitchell et al., 2001) of the plasma environment in the optical shadow of Mars, which found that the particle count rate dropped to near background levels forming “Plasma Voids” that occurred in association with strong crustal magnetic fields. In between these voids, a sharp

reappearance of electrons was found near local maxima in the radial field. Also, the observation of electrons with magnetosheath like energy spectra illustrated that the crustal fields were once connected to the IMF and this was interpreted to provide evidence for reconnection. The authors suggested that ‘magnetic cylinders’ on the nightside, emanating from the anomalies, may have prevented planetward-flowing solar wind plasma in the tail region from entering the closed field structures.

Mars is now orbited by another spacecraft, Mars Express, capable of studying the planet’s plasma environment by means of its ASPERA-3 plasma package. The main objective of ASPERA-3 is to study atmospheric loss via the solar wind interaction, using instruments that measure ions, electrons and energetic neutral atoms. Mars Express has been in orbit around Mars since December 25, 2003 and it follows a highly elliptical orbit with periapsis below 300km, and an apoapsis of $\sim 3.4R_M$.

In this paper we have used high resolution electron data taken from the ASPERA-3 Electron Spectrometer (ELS) on Mars Express, to observe the effects on space plasma around Mars by remanent magnetization in the Martian crust, and to examine differences between signatures on the day-side and night-side. We provide the first statistical evidence for the local time occurrences of intensifications and void signatures.

2. OBSERVATIONS

Our observations were made near closest approach during 144 orbits from 7th February, 2004 to 19th June, 2004. The choice of observing around the pericentre was to assure a one to one correspondence of unusual features in the ELS data to whether a model of the magnetic field of Mars predicated the presence of crustal magnetic fields. This was part of our preliminary study, and in the future we hope to look at higher altitudes on the dayside and nightside.

The electron spectrometer is a spherical top-hat electrostatic analyzer and a collimator system, and has an energy range 1eV-20keV with a $4^\circ \times 360^\circ$ field of view, divided into $16 \times 22.5^\circ$ sectors. The intrinsic energy resolution $\Delta E/E$ is 8%, although 24% data are used here. The energy sweep takes 4s, during which time ELS samples 128 energy levels. [For further details of the electron spectrometer, see the ASPERA-3 instrument section (Barabash et al., 2004) in the book “Mars Express: the scientific payload”].

We used a spherical harmonic model of the remanent magnetism of Mars (Cain et al., 2003) to obtain a proxy of magnetic field along the orbit of the spacecraft. We used the modelled values of magnetic field to find cases of local electrons which may be affected by crustal anomalies. The model is based on magnetic field measurements made by Mars Global Surveyor (MGS), and provides useful information between altitudes 400 km and 170 km. We use the model to produce three magnetic field components in a planetocentric spherical coordinate system; the radial field B_r which is positive away from the planet, the phi component B_ϕ and the theta component B_θ .

The Cain et al. model is built from MGS measurements which contain a combination of both internal magnetic fields (from crustal magnetism) and external fields. These external fields play a more dominant role on the dayside as the Gaussian spread of measurements used in developing the Cain et al. model are larger on the dayside, indicating a larger spread in the data caused by external fields. Therefore, the uncertainty in the dayside model values is larger precisely because the external field influence is not well determined. To improve confidence in the magnetic field proxy we have used a criterion which insures the predominance of the crustal magnetic field. The criterion was originally employed by Krymskii et al, 2003, on remote observations of the Martian night/day terminator and is defined by the following conditions

$$\frac{B^2}{8\pi} \geq p = 2K \times 10^{-8} \cos^2(\alpha) \text{ dyn/cm}^2, \alpha \leq 70^\circ \quad (1.1)$$

$$\frac{B^2}{8\pi} \geq p = 2 \times 10^{-9} \text{ dyn/cm}^2, \alpha \geq 70^\circ \quad (1.2)$$

where B is the magnetic field magnitude from crustal sources, α is the latitude and $K \approx 0.88$, and where the left hand term, of the magnetic field pressure applied by crustal sources is compared against p , the pressure exerted by the magnetosheath flow on mini-magnetospheres formed by crustal fields. The magnetosheath pressure is assumed on average to follow the Newtonian approximation given by Spreiter and Stahara, 1992. For further details on the derivation of the criterion see Krymskii et al, 2003.

Despite external fields not having a major affect on the nightside, Cain et al., 2003 found residuals in both the dayside and nightside observed field, when comparing the model predictions to the original MGS magnetic field data. In the Mars shadow there was a 4 - 6 nT scatter on all components, whereas the horizontal components on dayside ranged from 21 – 39 nT and a spread of 4 - 10 nT in the residuals was recorded for vertical component. These residuals could not be explained by external field effects, and to address this issue we will compare the MGS and Cain et al (2003) magnetic fields for the night-side data in the region of interest.

Figure 1a shows the ground track of Mars Express as the black line over an MGS magnetic field map produced at an altitude of 400 km (Connerney et al., 2001). The pass shown took place on 16th June, 2004 and occurred over the Martian terminator. The black and white dashed section shows where ELS made measurements at altitudes less than 400 km, and the arrow pointing at the orbital path marks where MEX ELS recorded the signature examined in this paper. This confirms that the instrument was over a region characterised by magnetic anomalies.

Figure 1b displays an ELS spectrogram in the first panel. Electron energy plotted in eV along the vertical axis, Universal Time (UT), Local Time (LT) and Solar Zenith Angle (SZ) is along the horizontal axis and the colour shows the differential energy flux of electrons. The angular distributions will be the subject of a further study. The second panel down shows the angle between the local zenith and the direction of the magnetic field. The third and fourth panel down show the proxy planetocentric magnetic field vector components

and the magnitude magnetic field calculated using the Cain model, the fifth panel shows the angle made by the plane of ELS with a line from the centre of the ELS to the centre of Mars (the Mars-ELS line), and the final panel shows the spacecraft altitude.

The spectrogram starts within the planetary plasma/electrons (area underneath the black bar on the left hand side). At 05:22:15 UT (21.17 LT), MEX ELS starts to record a reduced signal in electrons attributed to being in the Martial tail. The planetary plasma/electrons signal returns at 05:46:00 UT (04.08 LT), and ends at around 06:03:30 UT (07.77 LT). Next is a small transition region (the PEB) before the start of the magnetosheath and shocked solar wind plasma at 06:04:00 UT (07.85 LT) (area underneath the blue bar on the right hand side). In addition, photoelectrons appeared in the region of planetary plasma from 05:57:00 UT (07.11 LT) to 06:00:00 UT (07.47 LT), forming the medium density band on the spectrogram, during the time that the planetary plasma was in sunlight (solar zenith angle $SZ < 90.0$).

The feature of particular interest for this study is the intensification that occurred from around 05:48:45 UT (05.05 LT, 98.07 SZ), when Mars Express was at an altitude of 326.46 km. Recalling the data does not include actual measurements of magnetic field, we compare the spectrogram with the magnetic field model (3rd and 4th panel down). The Cain model predicts the radial component of the magnetic field varied between -174.0 nT and 28.5 nT, over the area where the intensification occurred. At the start of the event there was a magnetic field zenith angle of 27.41° , the angle of Mars in the ELS plane equalled 88.54° and there was a 23.7 nT magnetic field magnitude with a 21.0 nT radial component. The

event ended at 05:49:26 UT (05.40 LT), where the magnetic field zenith angle reached 103.57° , the angle of Mars in the ELS plane remained near 90° and there was a 26.4 nT magnetic field magnitude with a -6.2 nT radial component. The event being discussed shows signs of beginning at a minimum in the B zenith angle or what could be the location of a cusp. Other intensifications in the spectrogram at 05:47:13 (4.41), 05:53:35 (6.37), 06:00:37 (7.54) and 06:02:29 UT (7.65 LT) can also be seen to follow minimums and maximums of the B zenith angle, and there is also a suggestion of the major intensifications following the shape of the magnetic field magnitude.

Figure 2 displays the results of the Krymskii criterion for the 16th June, 2004 observation, with dynamic pressure along the vertical axis and using the same horizontal axis as in Figure 1b. The dotted curve shows the pressure of the mean solar wind conditions at the orbit of Mars and the solid line shows the pressure applied by the crustal magnetic fields. Figure 2 demonstrates that the criterion is more than satisfied from 05:44 UT (03.14 LT) to around 05:53:30 UT (06.45 LT), recalling that the event was recorded around 05:49:18 UT (05.39 LT).

In Figure 3 we compare the energy spectrum of differential energy flux from a point in the planetary plasma (solid line, labelled as point A on figure 1b at 05:59:09 UT, 07.36 LT) and another in the sheath (dashed line, labelled as point C on figure 1b at 06:12:36 UT, 08.40 LT), with four points in and immediately around the signature (dotted line, labelled as point B on figure 1b at 05:49:18 UT, 05.39 LT). Each spectrum is a time slice taken from the spectrogram in Figure 1b at points A, B and C respectively, where B represents

the four observations at the signature. Each figure from 3a to d, shows intensified plasma at the signature. The signature spectra show that at low energies (~ 4 eV to ~ 5 eV), the flux of signature particles bore a close resemblance to particles in the local region of planetary plasma which gave greater flux than particles from the sheath. At the energies of ~ 6 eV to ~ 12 eV, the signature particles in Figures 3a - d display higher fluxes than particles from the planetary plasma, possibly indicating acceleration of some of the planetary particles.

Figure 3a - d also reveal that, at energies between 20eV to 100eV where sheath particles had the highest flux, the signal of planetary electrons (point A in Figure 1b and the black spectra in Figure 3) was decreasing towards background noise levels, although there was still a strong signal of signature particles. This suggests that signature also contained material from the magnetosheath/ shocked solar wind, and this is supported in particular by Figure 3d which gives a clear indication of a sheath like spectrum within the signature, perhaps associated with a local distortion of the PEB. Figure 3c, also shows signs not observed at the other points in the signature, of accelerated sheath particles (>100 eV), possibly produced due to magnetic reconnection. The description given for Figure 3 shows that overall, the intensified signature event at 05:49:18 UT (05.39 LT) on 16th June, 2004 is mixture of particles in the sheath and the planetary plasma, however at other events we see either intensification of more ionospheric particles or sometimes of more sheath like particles.

Figure 4a shows the orbit path of Mars Express in relation to a night-time observation on 17th June, 2004. The black and white dashed section shows where ELS measurements are

available between altitudes 400 km - 170 km, and demonstrates that ELS was above a region containing magnetic anomalies. Here there are two arrows pointing at the orbital path, illustrating the period within which MEX ELS recorded signatures. Figure 4b displays the spectrogram of electrons and the modelled magnetic field pertaining to the above mentioned nightside pass. In comparison to the dayside, the spectrogram shows that the planetary plasma on the nightside had a far lower density, with planetary plasma ending at 22:24:50 UT (7.78 LT) while the magnetosheath and shocked solar wind plasma started at 22:26:40 UT (7.92 LT) (area underneath the blue bar on the right hand side). Here, there, were no planetary photoelectrons up to ~ 5.40 LT ($\sim 22:10$ UT) since the planetary plasma was not sunlit at the earlier times. However, in place of intensifications, is the intermittent disappearance or voids in planetary electrons from 21:54:40 UT (22.74 LT) to 22:04:20 UT (2.86 LT). The modelled magnetic field predicted that the voids coincided directly with an area where the magnetic field varied radially between -48 nT to -98 nT within the altitude range 400 - 170 km. In addition, four voids were observed centered at 21:55:31 (22.94 LT), 21:58:09 (23.80 LT), 22:00:25 (0.75 LT) and 22:02:42UT (1.93 LT) respectively, compared to four zero crossings of the radial field B_r , coinciding with a 90° local B zenith angle. We also observed electron flux spikes (c.f. Mitchell et al., 2001) at 21:54 (22.60), 21:56:30 (23.22) and 21:59UT (0.10 LT), which occurred immediately above local positive and negative peaks in the radial component of the crustal magnetic field and the local zenith angle.

We interpret the zero crossings of the radial field and where the local zenith angle becomes 90° to mark the tops of arches of the crustal magnetic field anomalies. In the intervening

cusps (maxima of radial field), particles may be travelling both towards and away from the planet. The incoming electrons are from the local plasma population: i.e. the solar wind/magnetosheath above the locally-distorted PEB on the dayside and the tail plasma on the night side. The cusp regions may be providing a location where enhanced escape of planetary plasma can occur. We anticipate that the more mobile electrons would escape first, setting up a local, field aligned, ambipolar electric field which could drag the ions away from the planet. The cusps may provide important concentrations of atmospheric loss via this mechanism, which we expect to be more significant on the day side. Further planned studies will compare the electron and ion data in detail to look for this effect.

Figure 5 shows the product of comparing the MGS magnetic field data (black line) in the Mars shadow with the Cain magnetic field model (dashed line). The MGS magnetic field is constructed from measurements made by the MGS MAG/ER instrument, at times when the location of the spacecraft coincided with the orbit path of MEX plotted in Figure 4a. The top three panels show the vector components of the planetocentric magnetic field in a spherical coordinate system and bottom panel shows the magnetic field magnitude, with altitude, latitude and longitude displayed along the horizontal axis. The vertical component or radial field and the magnitude field demonstrate a good agreement between MGS data and the Cain model. The theta component (that is horizontal to the planets spheroid) also shows a reasonable match between the Cain model and the MGS data, whereas the phi component makes the least convincing comparison. With only the phi component of the magnetic field model not conforming to the MGS data, the results of Figure 5 largely supports the use of the model in the analysis of the MEX ELS data.

We have examined spectrograms of the ELS electron data and the modelled magnetic field near periapsis for the interval 7th February, 2004 to 19th June, 2004. The signatures near to the anomalies have a wide variety of appearances. Our selection criteria were that the plasma region near a magnetic anomaly should have a different spectral signature to its surroundings. Some of the signatures showed intensifications over a wide energy range while some showed voids. During this time, 27 intensified signatures and 30 void signatures were recorded at altitudes between 400 km and 170 km, over 144 orbits.

For each signature, the local time of the spacecraft was recorded, and assigned to hourly bins. This enabled us to calculate the frequency of signatures in local time. The total period within which ELS observed between the altitudes of 400 km and 170 km during the 144 orbits was determined for each 1 hour bin. The signature occurrence rate has been normalized. For each bin, we found the number of signatures per hour and then divided it by the total duration of the observations (in hours). The results of this analysis are presented in Figure 6. This shows that intensifications have a broad distribution (from 03:00:00 LT to 15:00:00 LT), whereas void signatures show a narrower range in local time (23:00:00 LT to 04:00:00 LT). There were no data between 15:00:00 LT and 23:00:00 LT (see annotation on Figure 6), as the orbits used in the study did not enter the 400 - 170 km altitude range of this period in local time. We anticipate that this gap will be filled by Mars Express as the mission progresses but, already, our results concerning the day and night side signatures, and their differences are significant.

3. SUMMARY AND CONCLUSIONS

Observations made by the ASPERA-3 Electron Spectrometer, near magnetic anomalies in the Martian crust, have revealed that the space plasma around Mars undergoes significant changes in close proximity to remanent magnetic fields in the crust. Under such circumstances we have found that the local plasma either intensifies in flux or reduces. Intensified signatures have been observed to take place over a broad range in local time, from early daylight hours to late afternoon. Voids are the most severe case of a reduction in flux, and constitute the complete disappearance of electrons in local space. Voids have been observed to occur in a narrow range of local time and to be constrained to night-time hours.

A possible scenario could be that, on the dayside where the planetary plasma is sunlit and therefore the electron density is higher, additional solar wind penetration provides different energy spectra characterised by higher particle densities. The cusp structures distort the photoelectron boundary (PEB) region, and perhaps the IMB, locally. This could produce a focussing effect in the inflowing solar wind plasma, causing intensifications in the incoming and outgoing flux. On the nightside where there is no direct contact with solar wind plasma, there is a lower plasma density in the Martian tail, and the local distortions of the magnetic field and planetary plasma produce a much more visible reduction in electrons as the spacecraft enters a magnetic anomaly structure. Because only tail like plasma would enter at the cusps there are no noticeable intensifications on the night side.

We have suggested that the observed magnetic anomalies may be the sites of additional escape of planetary plasma/electrons. In further work we plan to extend the local time range of the signature events and explore the role they may play in enhanced escape processes.

Acknowledgments

The ASPERA-3 experiment on the European Space Agency (ESA) Mars Express mission is a joint effort between 15 laboratories in 10 countries, all sponsored by their national agencies. We thank all these agencies as well as the various departments/institutes hosting these efforts.

We wish to acknowledge NASA for ELS design, construction, operation and data analysis, which are supported by the NASA contract NASW00003 and UK's Particle Physics and Astronomy Research Council (PPARC) for support with PhD studentship funding.

We also wish to acknowledge the Swedish National Space Board for their support of the PI-institute and we are indebted to ESA for their courage in embarking on the Mars Express program, the first ESA mission to the red planet.

References

- Acuña, M. H., Connerney, J. E. P., Wasilewski, P., Lin, R. P., Anderson, K. A., Carlson, C. W., McFadden, J., Curtis, D. W., Mitchell, D., Rème, H., Mazelle, C., Sauvaud, J. A., d'Uston, C., Cros, A., Medale, J. L., Bauer, S. J., Cloutier, P., Mayhew, M., Winterhalter, D., Ness, N. F. 1998. Magnetic field and plasma observations at Mars: Initial results of the Mars Global Surveyor mission, *Science*, 279, 1676–1680.
- Acuña, M. H., Connerney, J. E. P., Wasilewski, P., Lin, R. P., Mitchell, D., Anderson, K. A., Carlson, C. W., McFadden, J., Rème, H., Mazelle, C., Vignes, D., Bauer, S. J., Cloutier, P., Ness, N. F. 2001. Magnetic field of Mars: Summary of results from the aerobraking and mapping orbits, *J. Geophys. Res.*, 106, 23403–23417.
- Barabash, S., Lundin, R., Andersson, H., Gimholt, J., Holmström, M., Norberg, O., Yamauchi, M., Asamura, K., Coates, A. J., Linder, D.R., Kataria, D.O., Curtis, C. C., Hsieh, K. C., Sandel, B. R., Fedorov, A., Grigoriev, A., Budnik, E., Grande, M., Carter, M., Reading, D. H., Koskinen, H., Kallio, E., Riihela, P., Säles, T., Kozyra, J., Krupp, N., Livi, S., Woch, J., Luhmann, J., McKenna-Lawlor, S., Orsini, S., Cerulli-Irelli, R., Mura, A., Milillo, A., Roelof, E., Williams, D., Sauvaud, J.-A., Thocaven, J.-J., Winningham, D., Frahm, R., Scherrer, J., Sharber, J., Wurz, P., Bochsler, P.. 2004. ASPERA-3: analyser of space plasmas and energetic ions for Mars Express, *Mars Express: the scientific payload*. ISBN 92-9092-556-6, 121 - 139
- Brain, D. A., Bagenal, F., Acuña, M. H., Connerney, J. E. P. 2003. Martian magnetic morphology: Contributions from the solar wind and crust, *J. Geophys. Res.*, 108, doi:10.1029/2002JA009482.

- Bertucci, C., Mazelle, C., Crider, D.H., Mitchell, D.L., Sauer, K., Acuña, M. H., Connerney, J. E. P., Lin, R.P., Ness, N.F., Winterhalter, D.. 2004. MGS MAG/ER observations at the magnetic pileup boundary of Mars: draping enhancement and low frequency waves, *Adv. Space. Res.*, 33, 1938-1944.
- Cain, J. C., Ferguson, B. B., Mozzoni, D. 2003. An $n = 90$ internal potential function of the Martian crustal magnetic field, *J. Geophys. Res.*, 102, doi:10.1029/2000JE001487.
- Coates, A.J., Wilken, B., Johnstone, A.D., Jockers, K., Glassmeier, K.-H. and Huddleston, D.E., 1990, Bulk properties and velocity distributions of water group ions at comet Halley: Giotto measurements, *J. Geophys Res*, 95, 10249-10260.
- Connerney, J. E. P., Acuña, M. H., Wasilewski, P. J., Kletetschka, G., Ness, N. F., Rème, H., Lin, R. P., Mitchell, D. 2001. The Global Magnetic Field of Mars and Implications for Crustal Evolution, *Geophys. Res. Lett.*, 28, 4015-4018.
- Krymskii, A. M., Breus, T. K., Ness, N. F., Hinson, D. P., Bojkov, D. I. 2003, Effect of crustal magnetic fields on the near terminator ionosphere at Mars: Comparison of in situ magnetic field measurements with the data of radio science experiments on board Mars Global Surveyor, *J. Geophys. Res.*, 108, doi:10.1029/2002JA009662.
- Mitchell, D. L., Lin, R. P., Mazelle, C., Rème, Cloutier, P.,H., Connerney, J. E. P., Wasilewski, Acuña, M. H., Ness, N. F. 2001. Probing Mars' crustal magnetic field and ionosphere with the MGS Electron Reflectometer, *J. Geophys. Res.*, Volume 106, 23419-23427.
- Spreiter, J. R., and S. S. Stahara, 1992, Computer modeling of the solar wind interaction with Venus and Mars, in *Venus and Mars: Atmosphere, Ionospheres, and Solar Wind Interactions*, *Geophys. Monogr. Ser.*, Volume 66, 345.

Winterhalter D., Acuña, M. H., and Zakharov, 2004. Mars' Magnetism and its interaction with the Solar Wind, *Space Science Revs.* Volume 111, Numbers 1-2

Figure captions

Figure 1a. Mars Express orbit path on 16th June 2004, over a map of the radial component of the magnetic field at 400 km altitude [Connerney et al., 2001]. The colour bar shows the field scaled to +/- 220 nT.

Figure 1b. Top panel - dayside energy-time spectrogram for upward electrons on 16th June 2004. Middle three panels - Magnetic field calculated using a model. Second panel down - magnetic field zenith angle. Third and fourth panel down - planetocentric magnetic field vector components and the magnitude magnetic field calculated using the Cain model. The fifth panel - angle made of the ELS plane with the line to the centre of Mars. Bottom panel - planetodetic altitude.

Figure 2. The criterion of crustal magnetic field dominance [Krymskii et al, 2003] for the observation on the 16th June, 2004, with dynamic pressure along the vertical axis. The pressure of the mean solar wind conditions at Mars is given by the dotted curve and the pressure of the crustal magnetic fields is given by the solid line.

Figure 3. Flux-energy spectrum comparing conditions in the planetary plasma, signature and the sheath on 16th June 2004. The solid line represents a point in the planetary plasma, the dotted line a point in the signature and the dashed line a point in the sheath. Each spectrum is a time slice taken from the spectrogram in Figure 1b at points A, B and C respectively. The four panels correspond to different slices of the signature event at 05:48:49, 05:48:53, 05:49:05 & 05:49:18 UT.

Figure 4a. Mars Express orbit path on 17th June 2004.

Figure 4b. Top panel - Mars nightside energy-time spectra for upward electrons on 17th June 2004. Middle three panels - Magnetic field calculated using a model. Bottom panel - planetodetic altitude.

Figure 5. Comparison of MGS magnetic field data (black line) with the Cain magnetic field model (dashed line) for the MEX orbit path on 17th June 2004. The top three panels – radial, theta and phi vector components of magnetic field and bottom panel shows the magnetic field magnitude. The horizontal axis gives altitude, latitude and longitude.

Figure 6. The normalisation of signature occurrences for intensified and void signatures, expressed in ‘Number of Signatures per Hour’.

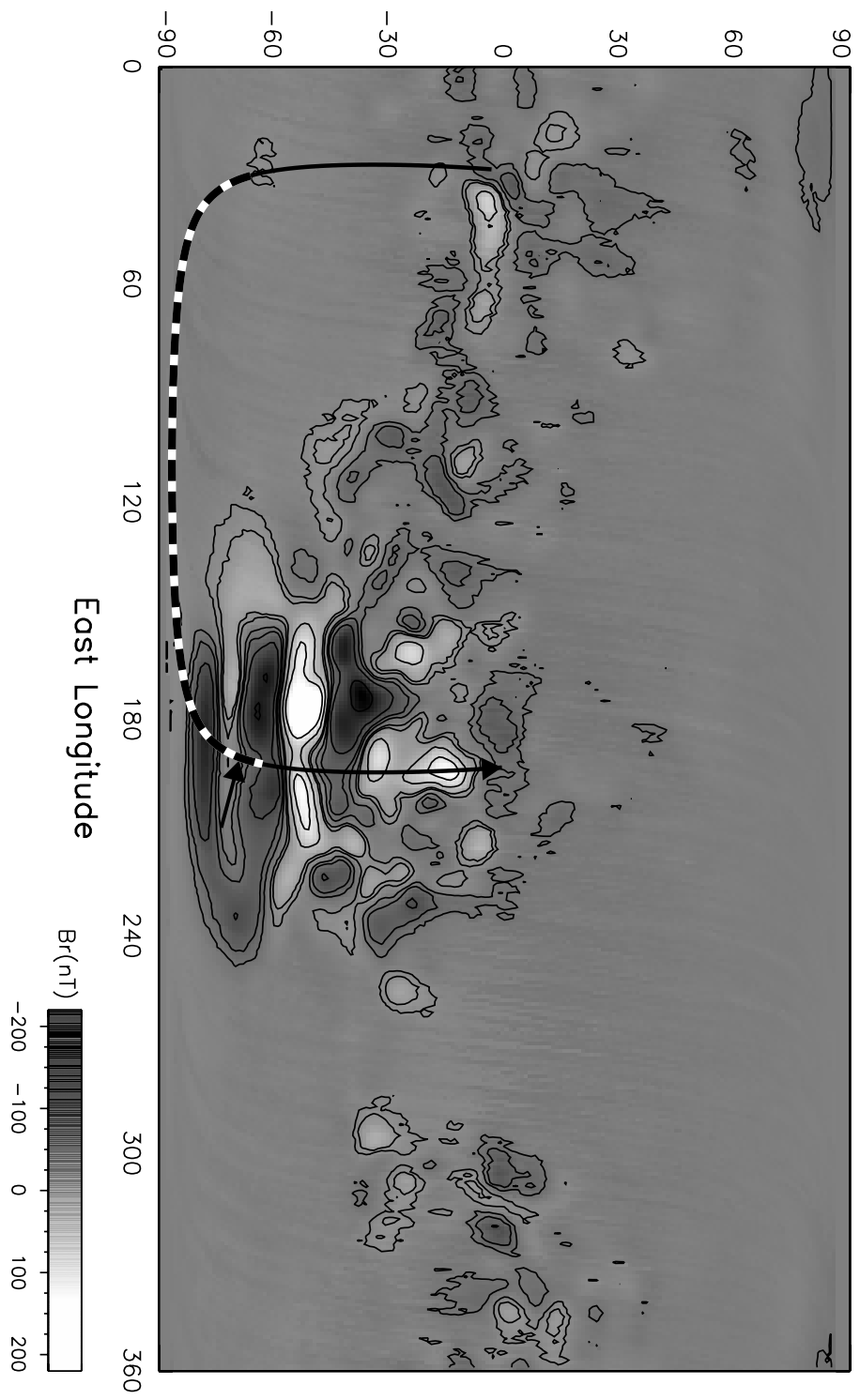


Figure 10 Soobich et al., Magnetic Anomalies

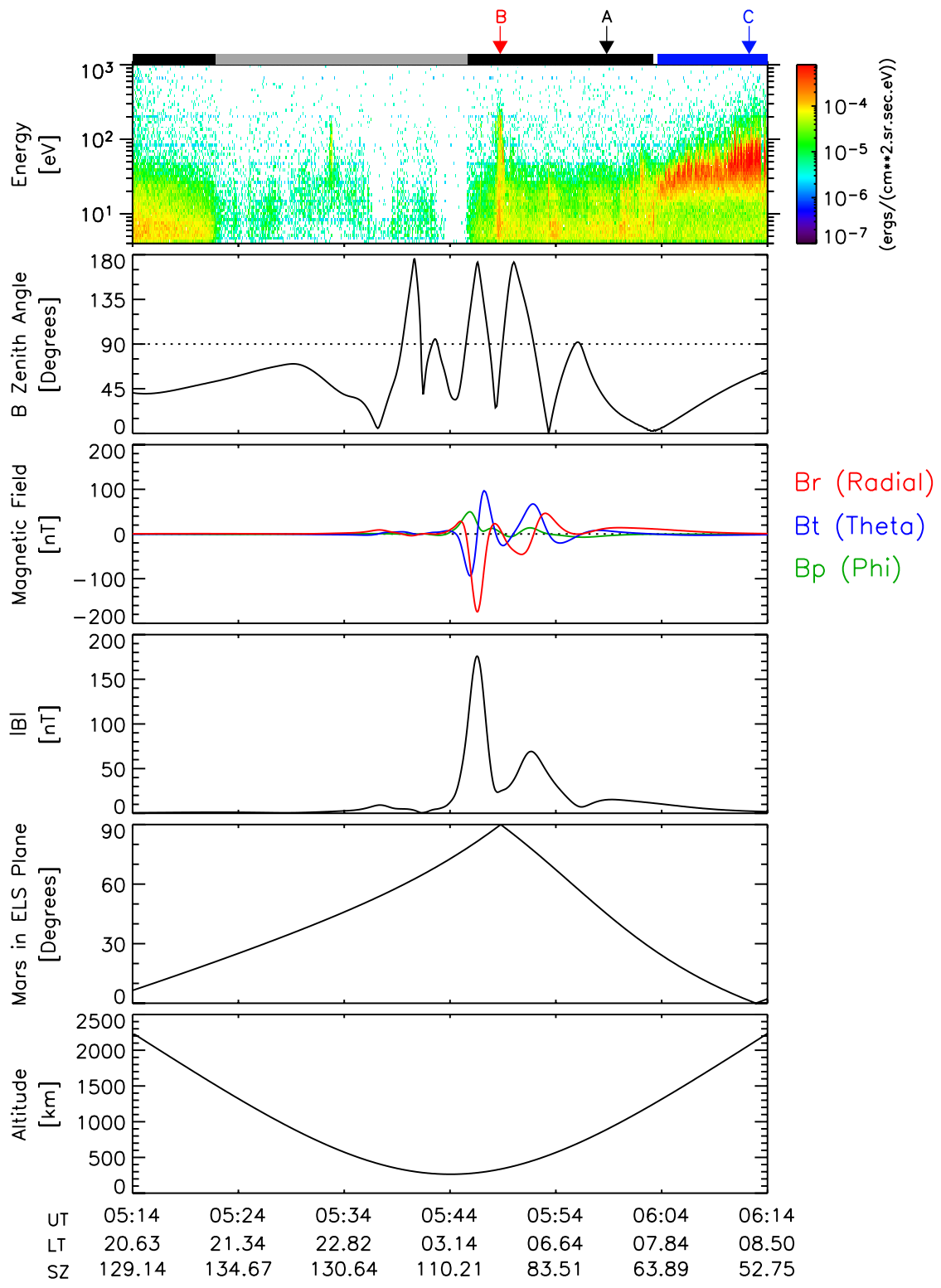


Figure 1b Soobiah et al., Magnetic Anomalies

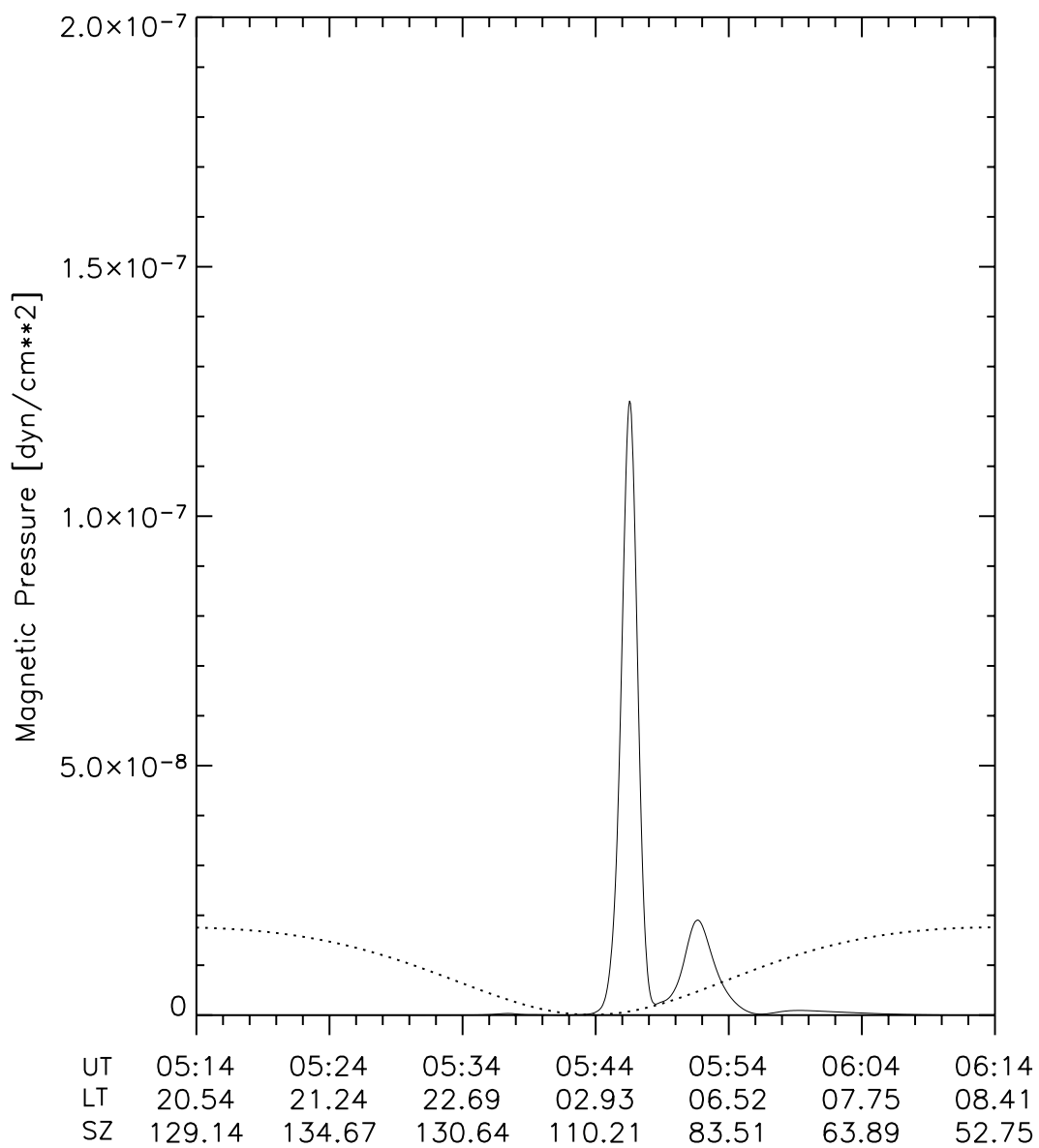


Figure 2 Soobiah et al., Magnetic Anomalies

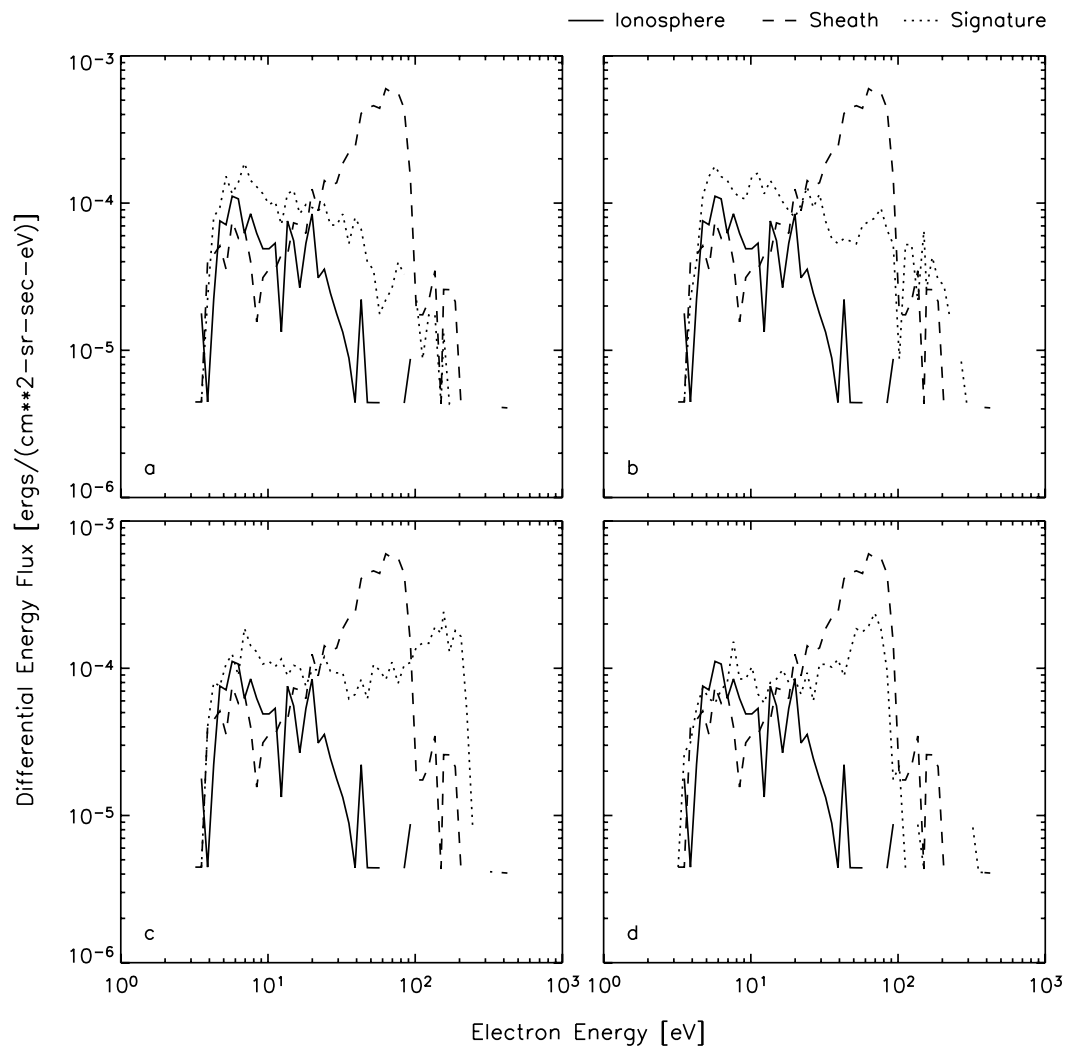


Figure 3 Soobiah et al., Magnetic Anomalies

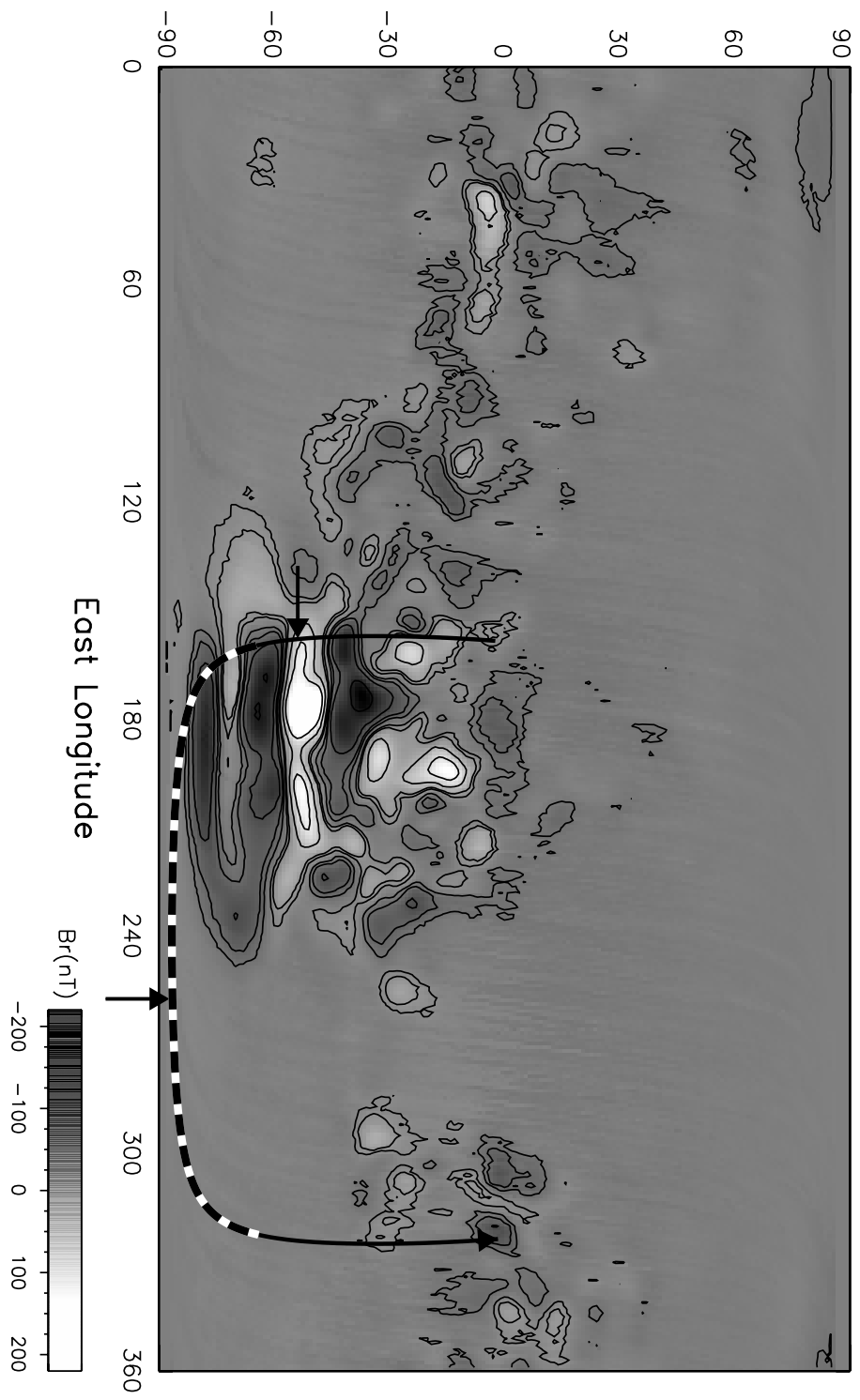


Figure 4a Soobich et al., Magnetic Anomalies

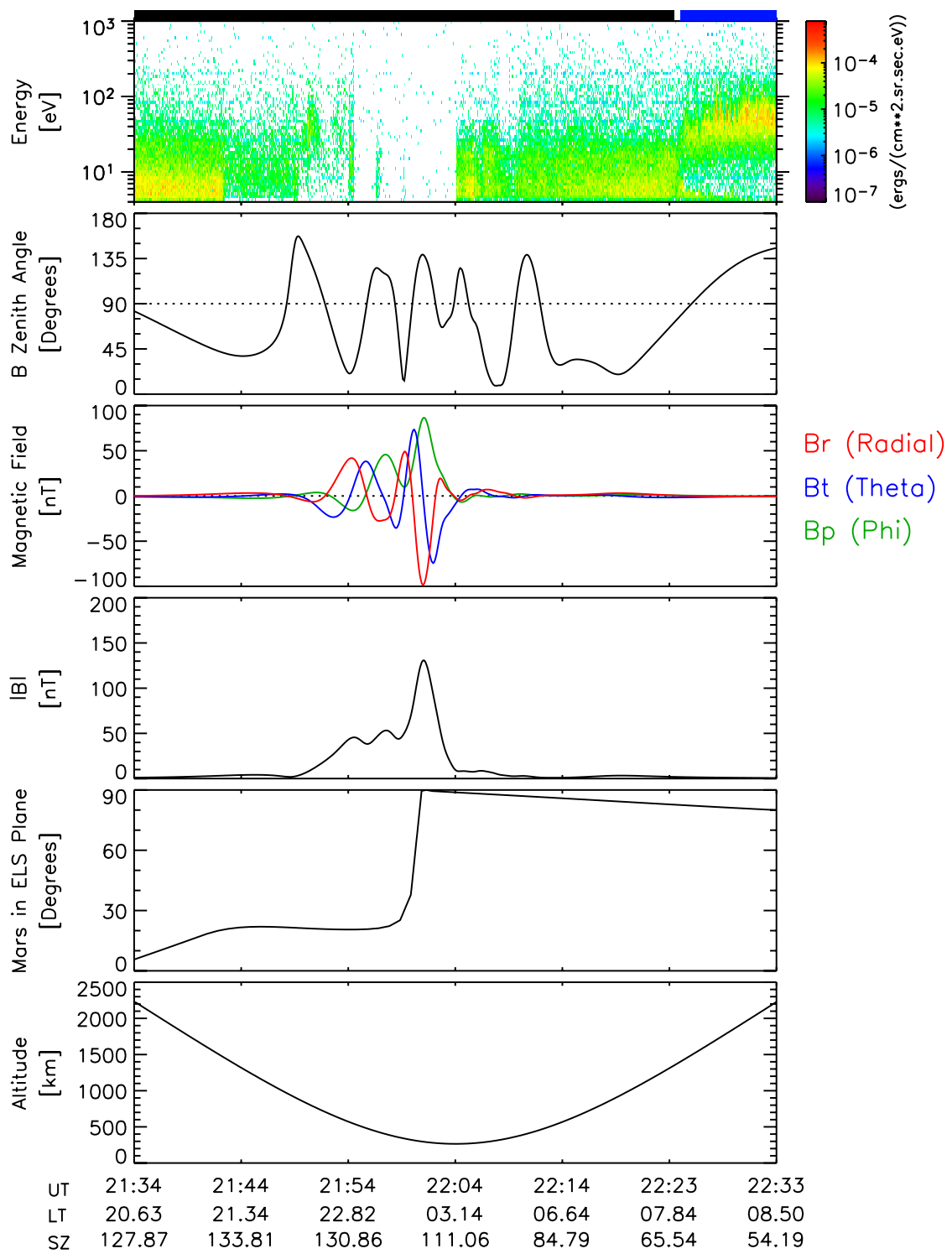


Figure 4b Soobiah et al., Magnetic Anomalies

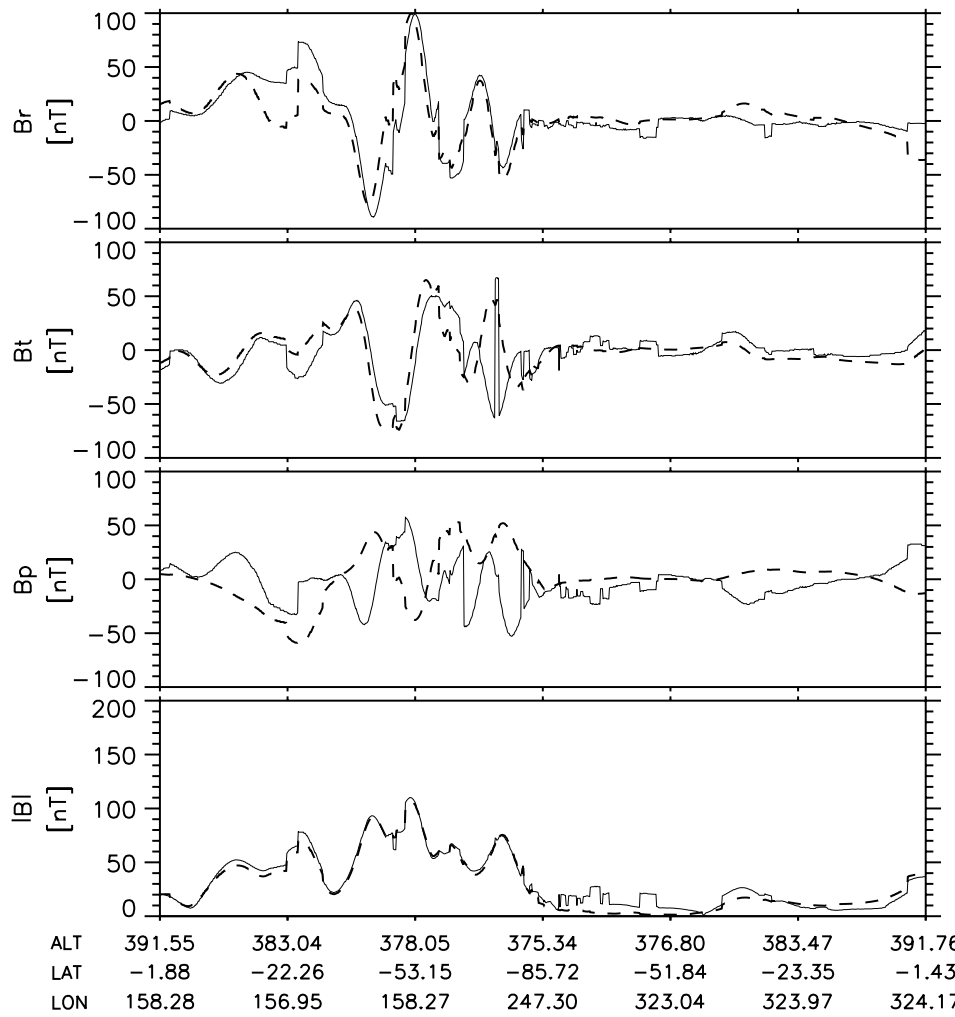


Figure 5 Soobiah et al., Magnetic Anomalies

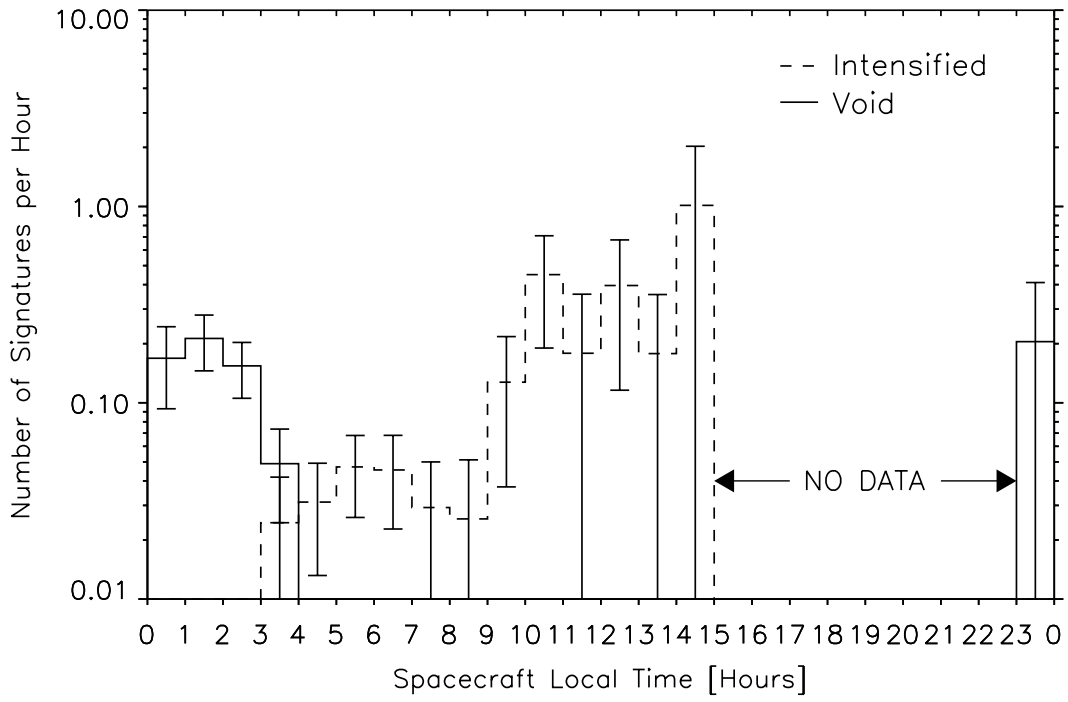


Figure 6 Soobiah et al., Magnetic Anomalies